

Guaianolide Sesquiterpene Lactones, a Source To Discover Agents That Selectively Inhibit Acute Myelogenous Leukemia Stem and Progenitor Cells

Quan Zhang,^{†,‡} Yaxin Lu,^{†,‡} Yahui Ding,^{†,‡} Jiadai Zhai,^{†,‡} Qing Ji,^{†,‡} Weiwei Ma,[†] Ming Yang,[†] Hongxia Fan,[†] Jing Long,[†] Zhongsheng Tong,[§] Yehui Shi,[§] Yongsheng Jia,[§] Bin Han,^{||} Wenpeng Zhang,^{||} Chuanjiang Qiu,^{||} Xiaoyan Ma,^{||} Qiuying Li,^{||} Qianqian Shi,[⊥] Haoliang Zhang,[†] Dongmei Li,[†] Jing Zhang,[†] Jianping Lin,[†] Lu-Yuan Li,[†] Yingdai Gao,^{*,†} and Yue Chen^{*,†}

[†]College of Pharmacy and The State Key Laboratory of Elemento-Organic Chemistry, Nankai University, and State Key Laboratory of Experimental Hematology, Institute of Hematology, Chinese Academy of Medical Sciences, Tianjin, People's Republic of China

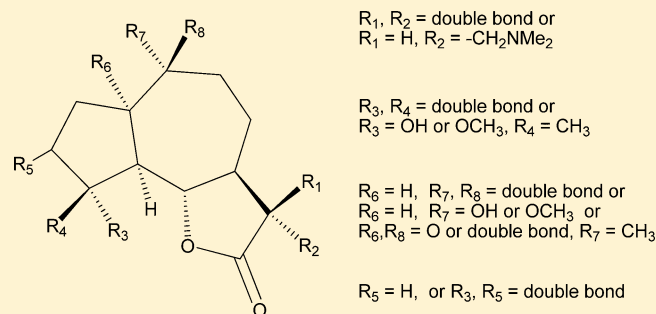
[§]Medical Department of Breast Oncology, Tianjin Medical University Cancer Institute and Hospital, Tianjin 300060, People's Republic of China

^{||}Accendatech Company, Ltd., Tianjin 300384, People's Republic of China

[⊥]College of Food Engineering and Biotechnology, Tianjin University of Science and Technology, Tianjin 300457, People's Republic of China

Supporting Information

ABSTRACT: Small molecules that can selectively target cancer stem cells (CSCs) remain rare currently and exhibit no common structural features. Here we report a series of guaianolide sesquiterpene lactones (GSLs) and their derivatives that can selectively eradicate acute myelogenous leukemia (AML) stem or progenitor cells. Natural GSL compounds arglabin, an anti-cancer clinical drug, and micheliolide (MCL), are able to reduce the proportion of AML stem cells (CD34⁺CD38⁻) in primary AML cells. Targeting of AML stem cells is further confirmed by a sharp reduction of colony-forming units of primary AML cells upon MCL treatment. Moreover, DMAMCL, the dimethylamino Michael adduct of MCL, slowly releases MCL in plasma and in vivo and demonstrates remarkable therapeutic efficacy in the nonobese diabetic/severe combined immunodeficiency AML models. These findings indicate that GSL is an ample source for chemical agents against AML stem or progenitor cells and that GSL is potentially highly useful to explore anti-CSC approaches.



A series of guaianolide SLs selectively ablate LSCs

■ INTRODUCTION

Cancer stem cells (CSCs) are able to differentiate into cancer progenitor cells and further into other cell types in a cancer context. It was first discovered that CD34⁺CD38⁻ leukemia stem cells could form tumors when transplanted into the SCID mouse model.¹ Many types of CSCs in solid tumors have been identified, including cancers of the brain, colon, ovary, pancreas, and prostate and melanoma.² It is now widely accepted that CSCs play a key role in carcinogenesis, cancer disease progression, relapse, and drug resistance.³ Conventional chemotherapies often lead to increased proportions of CSCs in cancers.^{4a} CSC-enriched cell populations not only demonstrate escalated resistance to chemotherapeutic agents and ionizing radiation,⁴ but also exhibit elevated tumor-forming potential.^{4a} However, chemical compounds that selectively inhibit CSC growth are rarely reported. Thus far, only a small number of compounds have been reported to selectively inhibit CSCs, including salinomycin,⁴ CITCO,⁵ repertaxin,⁶ MG-132,⁷ sulforaphane,⁸

and parthenolide (PTL)⁹ (Figure 1), but none of them are currently on the market as anticancer drugs. Chang reported that lapatinib treatment prevented the increase of tumorigenic cells in patients with locally advanced breast cancer and that a remarkable response rate was observed in a combination therapy approach using lapatinib, trastuzumab, and decetaxel.¹⁰

Novel anti-CSC compounds are highly desirable not only for therapeutic purposes, but also for mechanistic studies to understand stem cell biology. Although a number of intracellular signals and transcription factors such as Bmi-1, Notch, Sonic hedgehog, Wnt, NF-κB, and telomerase have been proposed to be potential targets for the modulation of CSC activities, these signaling pathways are shared with normal stem cells.¹¹ New entities that selectively regulate CSC activities are urgently needed as probes for signaling pathways specific to CSCs.

Received: July 20, 2012

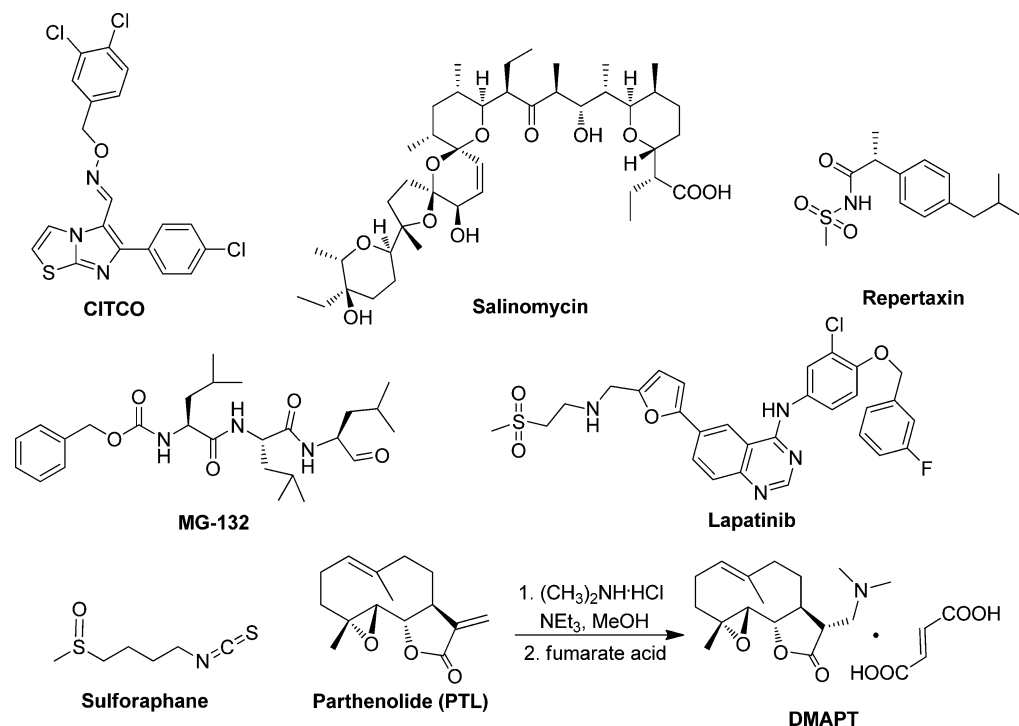


Figure 1. Structures of anti-CSC small molecules.

Parthenolide (PTL), a natural sesquiterpene lactone (SL) of 10,5-ring structure isolated from *Tanacetum parthenium* (Feverfew), is among the known anti-CSC molecules extensively studied.^{9,11–13} SLs are a family of chemical structures with more than 5000 members, many of which are used in traditional Chinese medicine for treatment of inflammation.¹⁴ Some studies indicate that the anti-inflammatory activities of SL are related to the inhibition of the transcription factor NF- κ B.¹⁵ PTL has been found to target NF- κ B, Stat3, HDAC, SERCA, and COX-2 in cancer cells.¹² The inhibition of NF- κ B and introduction of reactive oxidative species (ROS) appear to be important for PTL activity against CD34⁺CD38[−] leukemia stem cells (LSCs)^{9a,b} and breast cancer stem cells (BCSCs).^{9d} The water-soluble Michael adduct of PTL, DMAPT,^{9f} has entered clinical trial for cancer therapy.^{9g} However, PTL is unstable in both acidic and basic conditions.¹⁶

We have studied the activities of a series of SLs against AML stem or progenitor cells. Our data demonstrate that the 10,5-ring structure of PTL is not essential to the AML growth inhibition activity and that certain guaianolide sesquiterpene lactones (GSLs), a subtype of SLs characterized by a 5,7,5-ring structure,¹⁷ can selectively inhibit AML stem or progenitor cell growth. Moreover, a Michael adduct of micheliolide (MCL), dimethylaminomicheliolide (DMAMCL), exhibits remarkable therapeutic efficacy in AML NOD/SCID murine models.

RESULTS

Compound Syntheses. The compounds contain α,β -unsaturated carbonyl structures, including SLs and their derivatives, as shown in Figures 2–4. In comparison with PTL, several other commercially available SLs, including arglabin,¹⁸ dehydrocostus lactone (1), and costunolide (2), as well as artemisinin (3), which was reported to generate ROS to eradicate cancer cells,¹⁹ were evaluated for their anticancer activities. Since it is generally perceived that the α -methylene- γ -lactone moiety of SLs is responsible for their biological activities due

to its interaction with biological nucleophiles, such as cysteine sulfhydryl groups of target proteins, by a Michael-type addition,^{20–22} we also analyzed α -methylene- γ -lactone (4), itaconic anhydride (5), andrographolide (6), sarmentine (7), and a series of synthesized SL analogues (8–22) for their anticancer activities.

Activities against Cultured AML Cell Lines. The compounds were assayed against cultured AML cell line HL-60 and doxorubicin-resistant cell line HL-60/A (Table 1). Doxorubicin (DOX) and PTL were used as positive controls. The N₃ Michael adduct of PTL (14) demonstrated an activity profile similar to that of PTL, whereas the triazole derivatives of 14 (compounds 15–18) were inactive. Further analysis indicated that the N₃ adducts were completely converted to PTL in 3 h at physiological pH (7.4), whereas the inactive compounds 15–18 did not release PTL in 24 h under these experimental conditions. Additionally, the other 10,5-ring compound costunolide 2 was slightly less active than PTL; this suggests that the epoxide moiety of PTL is not essential for these biological activities.

Compounds 1, 8–10, 12–13, and 19–22 are a group of structures with a 5,7,5-ring. Among these compounds, 1, 8–10, 12, and 19–21 exhibited activities against HL-60 and HL-60/A comparable to that of PTL. Compound 13 (C10-OH-substituted) was less potent in comparison. However, the product with α -methylene reduction (compound 22) was completely inactive, indicating that α -methylene- γ -lactone is necessary for the anti-AML activity. Other non-SL natural products (compounds 4–7) and an open-ring SL derivative (compound 11) with Michael acceptors were basically inactive against HL-60 and HL-60/A cell lines. These results indicate that the 10,5- or 5,7,5-ring is important for SLs' anti-AML cell activities. For all the active SLs and derivatives, the activity against drug-resistant cell line HL-60/A was comparable to that against sensitive cell line HL-60. Compared with DOX, which exhibits an IC₅₀ of more than 100-fold against HL-60/A and

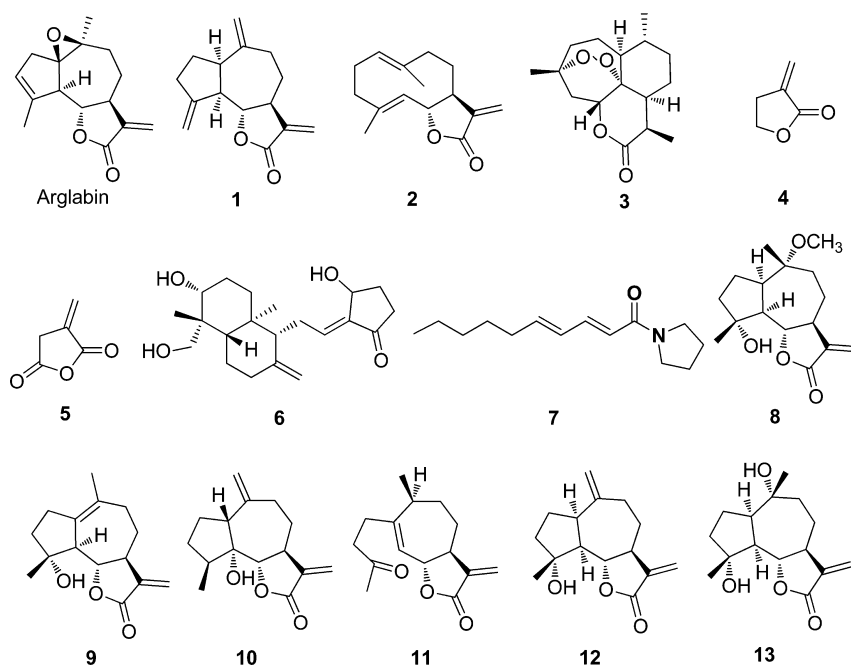


Figure 2. Structures of arglabin and compounds 1–13.

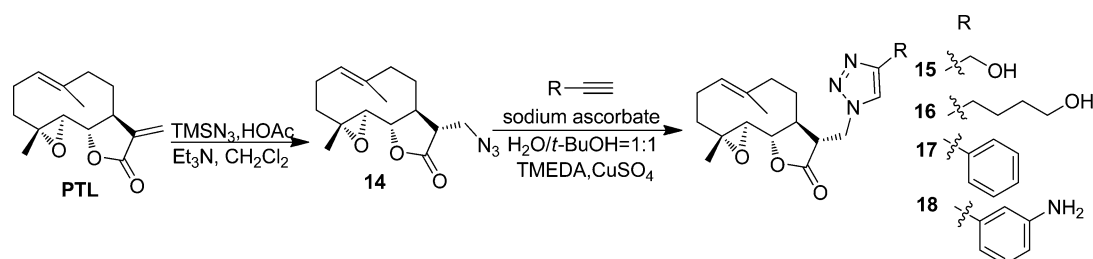


Figure 3. Synthesis of compounds 14–18.

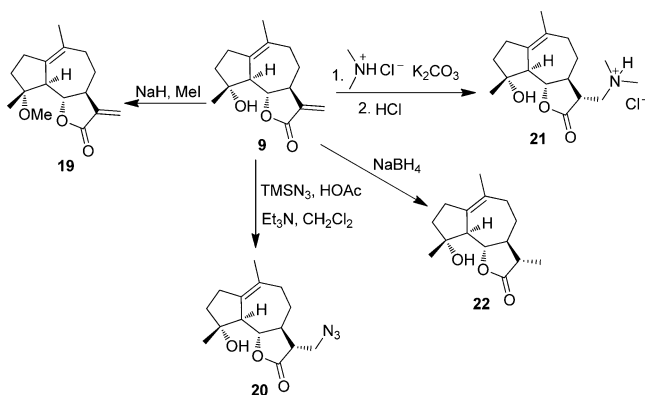


Figure 4. Synthesis of compounds 19–22.

HL-60, these active SLs are considerably more potent against drug-resistant AML cells.

Activities against Primary AML Cells and Stem/Progenitor Cells. Compounds 1, 2, 8–14, and 19–22 and arglabin were screened in the assay against primary total leukemia cells and leukemia stem/progenitor cells (CD34⁺) isolated from blood samples of AML patients (Table 2). The cell viability was determined by annexin labeling after 18 h of treatment. At 10 μ M, compounds arglabin, 1, 2, 9, 10, 12, 14, and 19–20 showed significant activity against leukemia stem/progenitor cells (CD34⁺-labeled). The cell viabilities of stem/

progenitor cells vs total leukemia cells after treatment with these compounds were (arglabin) 10.7% vs 20.0%, (1) 3.8% vs 6.4%, (2) 7.5% vs 13.4%, (9) 2.3% vs 8.4%, (10) 44.5% vs 49.7%, (12) 22.6% vs 30.6%, (14) 17.5% vs 22.8%, (19) 2.1% vs 10.8%, and (20) 11.2% vs 53.1%. These data indicate that the survival rates of AML stem/progenitor cells were lower than those of total leukemia cells upon treatment with these nine compounds. Again in comparison, treatment with DOX resulted in significantly higher survival rates for AML stem/progenitor cells vs total leukemia cells (115.0% vs 37.6% at 5 μ M and 49.1% vs 32.5% at 10 μ M), commonly observed also for other traditional anticancer agents.^{1–3}

Compounds arglabin, 1, 8–10, 10–13, and 19–22 are GSLs with characteristic 5,7,5-ring moieties. Since compound 9 (MCL) showed high potency and selectivity against leukemia stem/progenitor cells, it was used as a scaffold for a preliminary structure–activity relationship (SAR) study (Figure 5). The A-region-modified compound 22, derived from reduction of the 11,13-double bond of MCL, exhibited diminished inhibitory activity on both total leukemia cells and leukemia stem/progenitor cells (Table 2). This indicates that the α -methylene- γ -lactone is essential to the anti-AML activity, which is consistent with that of parthenolide.^{9f} The B-region-modified compounds 8, 10, 12, and 13 maintained activities against HL-60 and HL-60/A comparable to those of MCL (Table 1); however, their inhibitory activities against AML stem/progenitor cells were reduced. For example, compound 8 (C10-OCH₃-substituted),

Table 1. Biological Activities of Compounds against Cultured AML Cells (HL-60 and HL-60/A)^a

compd	HL-60 IC ₅₀ , μ M	HL-60/A IC ₅₀ , μ M	compd	HL-60 IC ₅₀ , μ M	HL-60/A IC ₅₀ , μ M
DOX ^b	0.05 \pm 0.01	6.7 \pm 0.8	11	>50	>50
PTL	3.7 \pm 0.1	4.1 \pm 0.4	12	9.4 \pm 2.6	9.9 \pm 2.1
1	5.3 \pm 1.7	3.7 \pm 0.9	13	21.9 \pm 3.2	17.9 \pm 1.2
2	7.7 \pm 1.2	5.8 \pm 1.4	14	4.3 \pm 0.7	5.9 \pm 0.55
3	>50	>50	15	>50	>100
4	35.0 \pm 3.9	28.8 \pm 5.4	16	>50	>100
5	>50	>50	17	>50	>100
6	27.0 \pm 1.5	23.3 \pm 6.4	18	>50	>100
7	>50	>50	19	9.9 \pm 0.9	10.2 \pm 0.14
8	9.4 \pm 0.8	11.2 \pm 1.6	20	6.2 \pm 1.7	6.7 \pm 2.1
9 (MCL)	5.5 \pm 1.4	6.2 \pm 2.2	21(DMAMCL)	17.2 \pm 1.1	21.5 \pm 2.0
10	4.5 \pm 0.8	6.4 \pm 0.3	22	>50	>50

^aAll values are the mean of three independent experiments. ^bDOX = doxorubicin, an anticancer agent used as a positive control.

Table 2. Biological Activities of Compounds against Total Cancer Cells and Cancerous Stem/Progenitor Cells (CD34⁺-Labeled) from AML Patient Blood Samples

compd	5 μ M				10 μ M			
	total		CD34 ⁺		total		CD34 ⁺	
	av % viable ^a	SD	av % viable ^a	SD	av % viable ^a	SD	av % viable ^a	SD
DOX	37.6 ^b	4.2	115.0 ^b	3.4	32.5 ^c	2.3	49.1 ^c	4.5
PTL	18.0	1.1	13.2	0.9	8.3	0.4	4.7	0.4
arglabin					20.0	1.5	10.7	0.9
1	6.1	0.3	2.9	0.2	6.4	0.2	3.8	0.3
2	25.8	1.1	18.8	1.0	13.4	0.5	7.5	0.1
8	96.5	0.7	95.8	0.7	75.2	0.3	76.3	0.5
9 (MCL)	11.7	2.2	4.2	2.2	8.4	0.5	2.3	0.6
10	70.7	0.5	67.9	1.1	49.7	2.6	44.5	2.4
11	83.2	1.4	81.5	1.1	72.0	0.7	70.9	0.4
12	61.6	1.0	53.7	2.5	30.6	1.3	22.6	1.8
13	88.5	6.6	84.9	8.9	89.9	2.9	84.8	2.7
14	31.5	0.9	28.4	1.1	22.8	3.2	17.5	5.7
19	34.1	0.9	25.5	1.5	10.8	0.5	2.1	0.2
20	64.3	9.9	26.3	3.3	53.1	1.0	11.2	1.0
21(DMAMCL)	77.6	3.0	72.9	2.7	64.9	0.1	60.4	0.1
22	85.0	1.4	83.1	1.5	70.8	1.2	74.4	1.0

^aViability normalized to untreated controls. ^bDOX was treated with 0.1 μ M. ^cDOX was treated with 0.5 μ M.

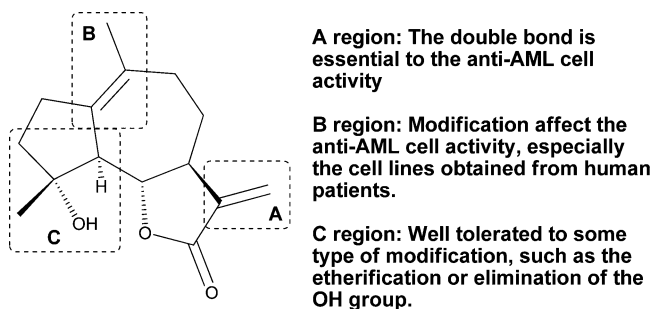


Figure 5. Preliminary structure–activity relationship of 5,7,5-ring-type SLs.

a GSL modified at the B-region with high activity against HL-60 (IC₅₀ = 9.4 \pm 0.8 μ M) and HL-60/A (11.2 \pm 1.6 μ M) cell lines, showed weak potency against human AML stem and progenitor cells (76.3% viable CD34⁺ cells at a concentration of 10 μ M). This suggests that certain types of modifications in the B-region affect the anti-AML cell activity, especially the AML stem and progenitor cells. For the C-region, methylation of the hydroxyl group of MCL (compound 19)

largely maintained activity against AML stem/progenitor cells (2.1% viable CD34⁺ cells at 10 μ M) comparable to that of MCL (2.3% viable CD34⁺ cells at the same concentration). Argabin, the compound with the hydroxyl group eliminated, also showed high potency against leukemia stem/progenitor cells (10.7% viability at 10 μ M). These findings suggest that the hydroxyl group can accommodate certain types of modifications, such as etherification or elimination. Compound 1, dehydrocostus lactone, which has an olefin in the C-region and a methylene moiety in the B-region, demonstrated activities against both total leukemia cells and leukemia stem/progenitor cells comparable to those of MCL, but was unstable at room temperature. We therefore selected MCL and argabin for further evaluation.

MCL and Argabin Selectively Inhibit Leukemia Stem Cells. We analyzed the effects of PTL, MCL, and argabin treatment on CD34⁺CD38[−] AML cells. The percentages of CD34⁺ and CD34⁺CD38[−] cells in all surviving cells in response to these compounds at 10 μ M are given in Table 3. The proportions of stem cells in all living cells decreased by 2.6-, 1.9-, and 5.3-fold for PTL, argabin, and MCL treatment, respectively, compared with those in the vehicle-treated controls. This finding indicates that

Table 3. Proportion of CD34⁺ and CD34⁺CD38⁻ Cells in Overall Living Cells in Response to Compounds PTL, Arglabin, and MCL at a Concentration of 10 μ M

compd	CD34 ⁺ (%)	fold decrease ^a	CD34 ⁺ CD38 ⁻ (%)	fold decrease ^b
control	57.9 \pm 2.6	1	12.1 \pm 3.3	1
PTL	15.1 \pm 4.2	3.8	4.6 \pm 0.8	2.6
arglabin	31.7 \pm 0.7	1.8	6.4 \pm 0.1	1.9
MCL	17.8 \pm 2.5	3.2	2.3 \pm 0.9	5.3

^aRatio of the percentage of CD34⁺ cells compared to that of the control. ^bRatio of the percentage of CD34⁺CD38⁻ cells compared to that of the control.

the three compounds selectively eradicate AML progenitor/stem cells and stem cells.

MCL Selectively Inhibits AML-Subtype Cell Lines Obtained from Human Patients. We further analyzed PTL and MCL against primary AML cells isolated from blood samples of AML patients (Figure 6) using methods as described.^{9a} At a concentration of 10 μ M MCL, lower cell viability was observed for the CD34⁺ subtype than that for total AML cells. This indicates that MCL, similar to PTL, may selectively inhibit AML progenitor/stem cells.

Effect of MCL on Colony-Forming of AML Cells. The mononuclear cells from cord blood of AML patients were cultured in serum-free Iscove's modified Dulbecco's medium (IMDM) for 18 h in the presence of DOX, PTL, and MCL, respectively. Since DOX has a much lower IC₅₀ concentration against AML cells than PTL and MCL (Table 1), we used low concentrations of DOX (0.05 and 0.1 μ M) to ensure a comparable proportion of AML cells survived after drug treatments.

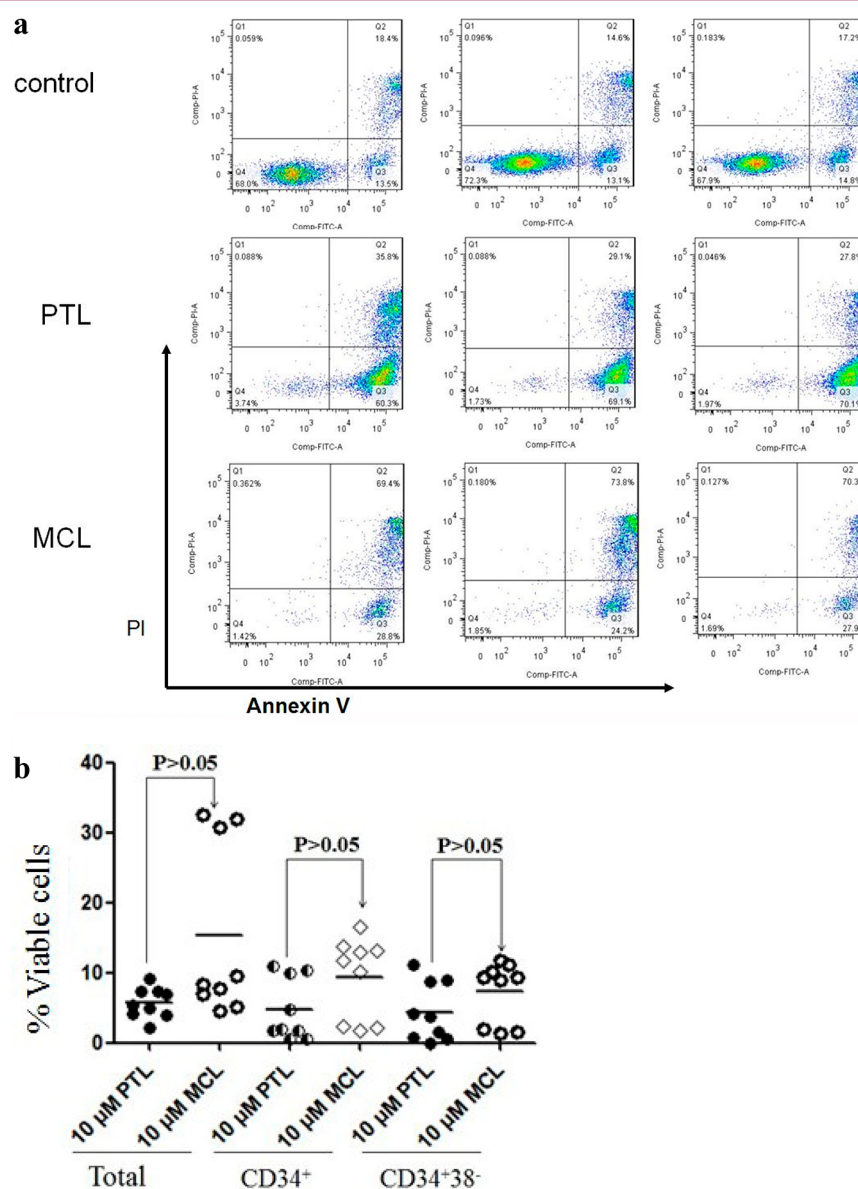


Figure 6. Analysis of PTL- and MCL-induced apoptosis with flow cytometry. (a) Viability of CD34⁺ cells in a typical leukemia specimen in response to compounds PTL and MCL. Q1 indicates the necrotic cells, Q2 indicates the late apoptosis of the leukemia cells, Q3 indicates the early apoptosis of the leukemia cells, and Q4 indicates the viability of leukemia cells. From the pictures we can conclude that the cells of Q4 were reduced strongly after the treatment of PTL and MCL, which indicated the viabilities of the cells were strongly reduced. (b) Viability (Q1) of total cells, CD34⁺-labeled cells, and CD34⁺CD38⁻-labeled cells in various leukemia specimens in response to compounds PTL and MCL at 10 μ M.

The numbers of colonies were scored after 15–20 days of culture. The colony-forming units (CFUs) of DOX-treated cells were 165–170 (Figure 7), approximately 25% reduction

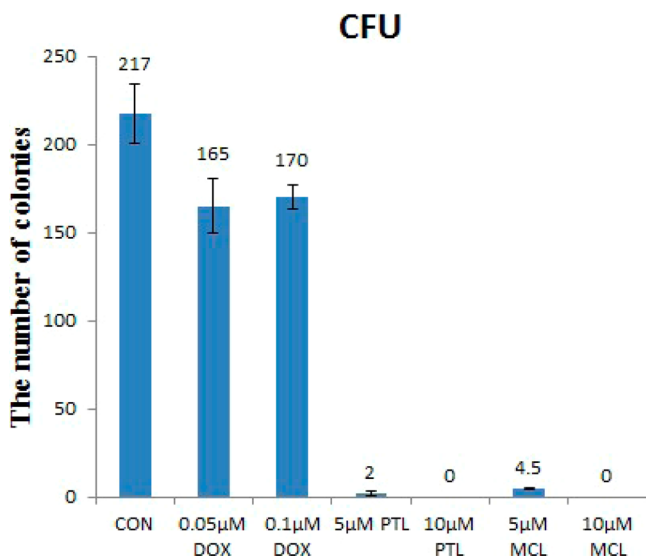


Figure 7. Reduction of methylcellulose colony-forming in response to compounds DOX, PTL, and MCL.

compared with that of the vehicle control. However, the CFUs after PTL or MCL treatment were dramatically reduced on average to 4.5 or lower. The significant reduction of AML CFUs by PTL, but not that by MCL, was reported previously by other investigators.^{9a} These findings indicate that MCL, similar to PTL, preferentially targets AML progenitor cells.

Effect of MCL on Normal Blood Cells and Hematopoietic Stem/Progenitor Cells. An *in vitro* apoptosis assay was used to evaluate the effect of MCL on normal hematopoietic stem/progenitor cells (HSCs). The percentage of apoptotic cells was normalized to that of the vehicle control (Figure 8a). MCL showed less effect against normal hematopoietic stem/progenitor cells (CD34⁺ cells) than PTL ($p < 0.05$, Figure 8b). In other words, MCL is potentially safer than PTL at the cell level.

Ex Vivo Biological Activity of MCL in an AML Murine Model. We investigated the selectivity of MCL against AML stem cells in an *ex vivo* experiment by using a NOD/SCID murine model. Freshly isolated primary AML cells were treated with saline, PTL, and MCL, respectively, for 18 h, and then the same numbers of surviving cells were intravenously injected into

NOD/SCID mice. The animals were sacrificed after 8 weeks, and the percentage of human mononuclear cells (with a CD45⁺ marker) in the bone marrow and spleen was determined (Figure 9). Detection of CD45⁺ cells indicates human leukemia cells engrafted, and then it can be concluded that both PTL and MCL treatments substantially reduced the ability of leukemia stem cells to engraft in the animals in the bone marrow ($p < 0.01$, Figure 9a) and the spleen ($p < 0.01$, Figure 9b). Human cancer cells were detected in a significant number in the spleen of the control group, but hardly were detectable in PTL- or MCL-treated groups. This finding demonstrates that both PTL and MCL can reduce the cancer-initiating capability of AML cells.

Stability in Mouse Plasma. The half-lives of PTL and MCL in mouse plasma are given in Table 4. The half-life of PTL is only 0.34 h, whereas that of MCL is 2.64 h. These *in vitro* studies suggest that the structure optimization from PTL to MCL has improved the compound physiological stability by 7-fold; thus, it is likely to be more stable *in vivo*.

Transformation from Prodrug to Active Drug. With the similar method to prepare DMAPT from PTL,^{9f} we synthesized the dimethylamino Michael adduct of MCL, DMAMCL, to improve aquatic solubility (Figure 4, compound 21). DMAPT and DMAMCL were analyzed in HEPES buffer as well as in plasma. In HEPES with pH lower than 5.0, DMAPT and DMAMCL were stable, and no significant amount of PTL or MCL was released in 5 days (data not shown). However, in HEPES with pH 7.4, DMAPT was converted to PTL rapidly, while DMAMCL released MCL slowly but consistently (Figure 10). In plasma, DMAMCL and DMAPT transformed to MCL and PTL, respectively (Figure 11). The half-life of DMAMCL is much longer; thus, MCL was continuously released from DMAMCL steadily for more than 8 h. In contrast, the concentration of PTL released from DMAPT decreased to 0.1 μg/mL in 2.5 h. These data indicate that DMAMCL has superior *in vivo* kinetic properties compared to DMAPT as a prodrug, and this advantage of DMAMCL might lead to better therapeutic potential.

Pharmacokinetic Study of DMAMCL in Mice. The plasma concentration–time curves for DMAMCL and MCL after a single 150 mg/kg per os (po) dose of an aqueous solution of DMAMCL in mouse are given in Figure 12a. The pharmacokinetic parameters determined with a noncompartmental model are given in Table 5. Having quickly reached a peak, the plasma concentrations of both DMAMCL and MCL declined gradually. Thus, DMAMCL was constantly transformed into MCL *in vivo*. These findings indicate that DMAMCL can sustain the release of

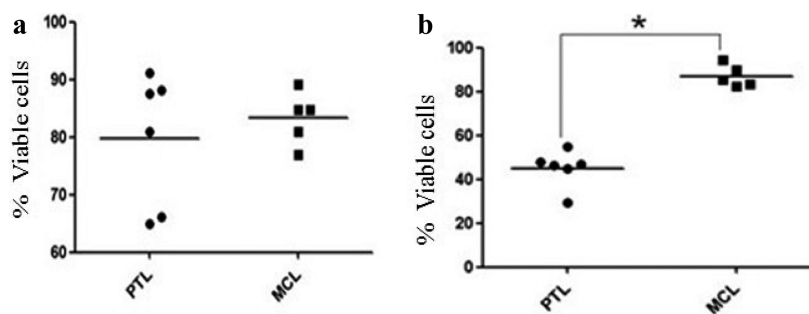


Figure 8. Normal specimens in response to compounds PTL and MCL. (a) Viability of total normal cells (mononuclear cells from the umbilical cord blood samples) in response to compounds PTL and MCL at a concentration of 5 μM. (b) Viability of CD34⁺-labeled normal cells (stained by the antibody CD34-allophycocyanin for 30 min) in response to compounds PTL and MCL at a concentration of 5 μM (the asterisk indicates $p < 0.05$).

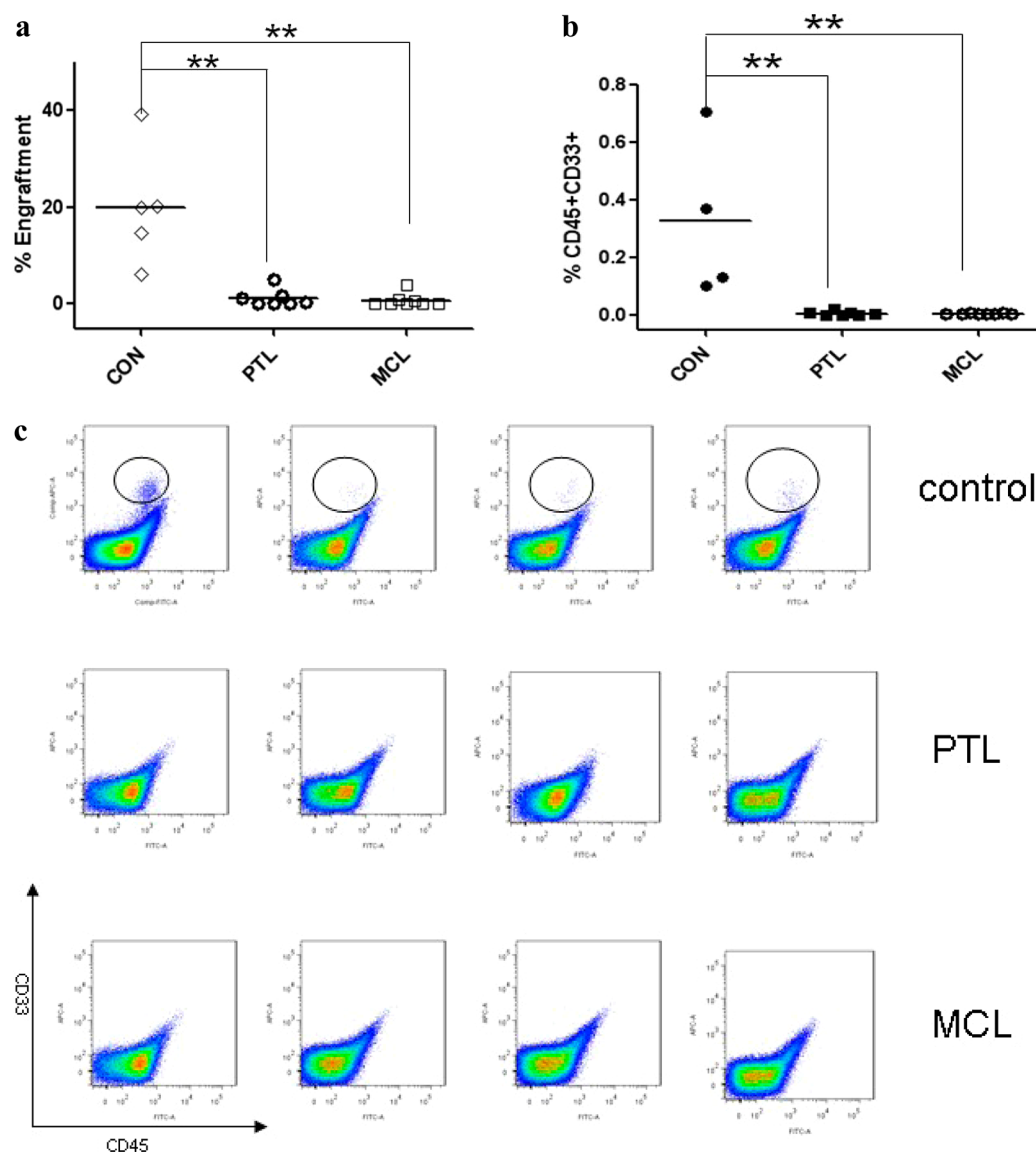


Figure 9. Analysis of CD45⁺CD33⁺ cells in bone marrow and spleen with flow cytometry. Percentage of CD45⁺ cells in the bone marrow (two asterisks indicate $p < 0.01$) (a) and CD33⁺CD45⁺ cells in the spleen (two asterisks indicate $p < 0.01$) (b) in NOD/SCID mice, which were sacrificed 8 weeks after transplantation with the primary AML cells pretreated with PTL and MCL for 18 h. Each \diamond , \circ , \square , \bullet , or \blacksquare symbol represents a single animal analyzed at 8 weeks after transplantation. The mean percentage is indicated by the horizontal bars. (c) Analysis of typical spleen samples with flow cytometry. The CD33⁺CD45⁺ cells (in the circles) were obviously in the spleen in the control, but in PTL- and MCL-treated groups, the CD33⁺CD45⁺ cells were nearly invisible in the spleen.

Table 4. Half-Life of PTL and MCL in Mouse Plasma^a

	PTL	MCL
$t_{1/2}$, h	0.34	2.64

^aThe starting concentration of PTL and MCL was 1 mg/mL.

MCL, resulting in an effective concentration range of the blood level of MCL for a relatively long time.

The pharmacokinetics of DMAMCL was studied by intravenous injection at 100 mg/kg (Figure 12b), and the pharmacokinetic parameters are given in Table 6. The oral bioavailability of DMAMCL was also determined and found to be 75%. These data suggest that the basic pharmacokinetic properties of DMAMCL make it sufficiently promising as a prodrug.

In Vivo Efficacy Study of DMAMCL in the AML NOD/SCID Murine Model. The potency and selectivity of DMAMCL were determined in vivo using an AML NOD/SCID murine

model. The model was established by tail vein injection of primary AML cells isolated from AML M5 patients. After 8 weeks postinoculation, 100 mg/kg DMAMCL or 100 mg/kg DMAPT was orally administered once every other day for a total of seven doses. As a control experiment, 1 mg/kg DOX was administered via tail vein every other day for a total of four doses. As shown in Figure 13b, the average life span of the DOX-treated animals was 22 days, which is shorter than that of the untreated control group (43 days). Similar results for DOX treatment were observed in the literature,²³ and this is likely due to sensitivity of the NOD/SCID mice to DOX toxicity. The average life spans for DMAPT- and DMAMCL-treated groups were 66 and 63 days, respectively. Moreover, 17% of DMAPT-treated (1/6) and 33% of DMAMCL-treated (2/6) animals remained alive on day 85 postinoculation. These three animals were sacrificed, and the bone marrow was analyzed. The percentage of CD45⁺CD33⁺ human AML cells in the

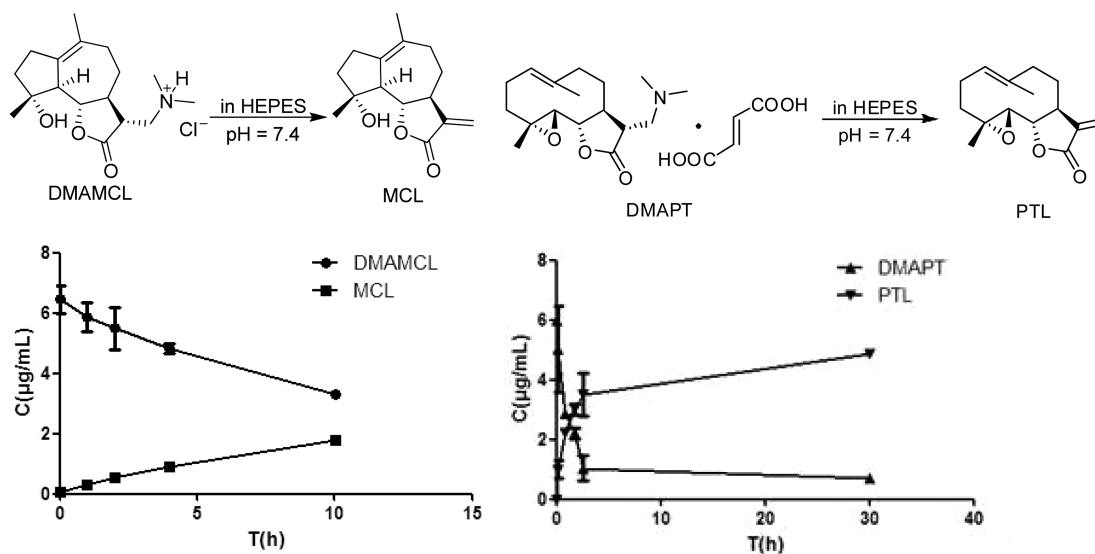


Figure 10. Concentration–time curve of DMAMCL (●), MCL (■), DMAPT (▲), and PTL (▼) in HEPES of pH 7.4 (mean \pm SD, $n = 4$).

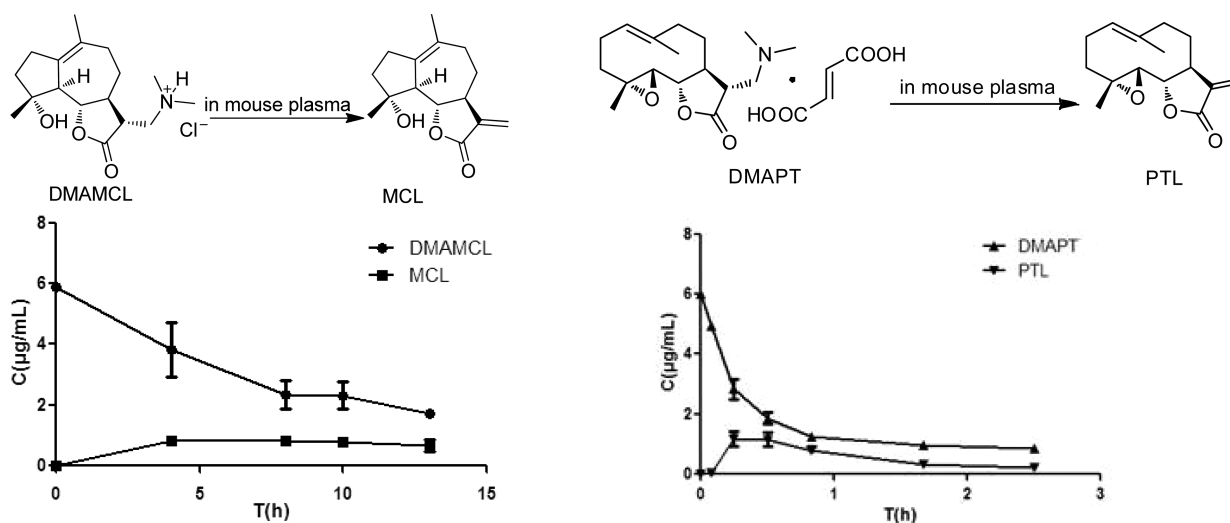


Figure 11. Concentration–time curve of DMAMCL (●), MCL (■), DMAPT (▲), and PTL (▼) in mouse plasma (mean \pm SD, $n = 4$).

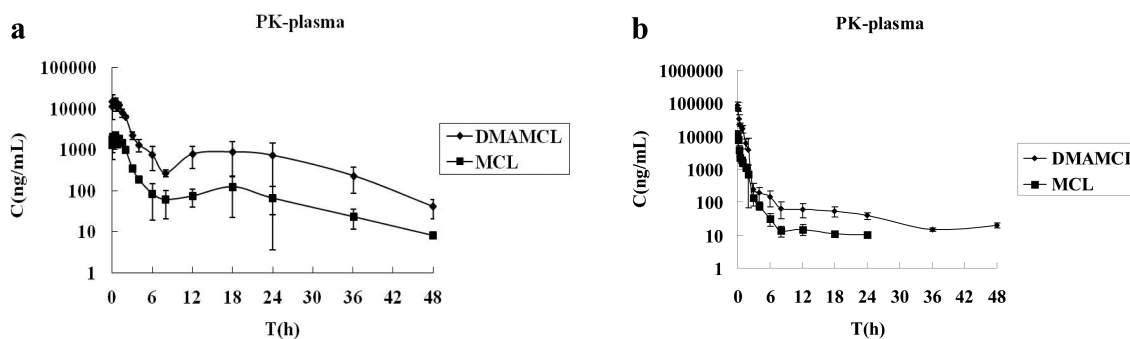


Figure 12. PK study of a DMAMCL aqueous solution given po administration and iv administration. (a) DMAMCL (◆) and MCL (■) plasma concentration–time curve in mouse after a single po administration of drug (150 mg/kg) (mean \pm SD, $n = 5$). (b) DMAMCL (◆) and MCL (■) plasma concentration–time curve in mouse after a single iv administration of drug (100 mg/kg) (mean \pm SD, $n = 5$).

DMAPT-treated mouse was 35%, whereas those in the two DMAMCL-treated animals were 0.005% and 0.12%, indicating a basically “disease-free” state for these animals at the end of the study. Furthermore, the average percentage of CD45⁺CD33⁺ cells in DMAMCL-treated mice was lower than that of

DMAPT-treated mice (Figure 13a), suggesting that DMAMCL is superior to DMAPT as a prodrug.

In another experiment, NOD/SCID mice were engrafted with acute mixed-lineage leukemia cells and then treated with the same drug treatment protocol as stated above. All animals were

Table 5. Pharmacokinetic Parameters of DMAMCL and MCL after a Single po Administration of Drug Aqueous Solution (150 mg/kg) (mean \pm SD, $n = 5$)

param	unit	DMAMCL	SD	MCL	SD
AUC ^a (0– t)	ng/mL·h	49633.6	10851.9	6632.3	830.1
AUC(0– ∞)	ng/mL·h	50326.8	10324.7	6715.2	800.6
AUMC ^b (0– t)		460496.6	222944.3	51360.6	17748.2
AUMC(0– ∞)		507542.7	187204.4	56375.6	16132.2
MRT ^c (0– t)	h	8.85	2.75	7.59	1.77
MRT(0– ∞)	h	9.85	1.86	8.28	1.52
$t_{1/2}$	h	9.82	5.72	7.92	2.51
T_{\max}	h	0.19	0.19	0.36	0.20
CL ^d	L/h/kg	3.08	0.63	22.59	2.6
V	L/kg	47.38	35.88	265.27	108.6
C_{\max}	ng/mL	18966.9	3136.5	2607.6	436.7

^aArea under the curve. ^bArea under the first moment of the plasma concentration–time curve. ^cMean retention time, MRT = AUMC/AUC. ^dTotal body clearance.

Table 6. Pharmacokinetic Parameters of DMAMCL and MCL after a Single iv Administration of Drug Aqueous Solution (100 mg/kg) (mean \pm SD, $n = 5$)

param	unit	DMAMCL	SD	MCL	SD
AUC ^a (0– t)	ng/mL·h	43943.7	5381.6	5489.4	638.2
AUC(0– ∞)	ng/mL·h	44812.3	6084.5	5847.3	628.1
AUMC ^b (0– t)		66198.7	9444.2	8135.3	1078.1
AUMC(0– ∞)		167803.6	151987.5	37846.8	47828.8
MRT ^c (0– t)	h	1.51	0.09	1.49	0.15
MRT(0– ∞)	h	3.52	2.57	6.34	7.90
$t_{1/2}$	h	18.92	7.36	12.66	5.67
CL ^d	L/h/kg	2.26	0.28	17.25	1.72
V	L/kg	88.18	56.37	533.45	509.56
C_{\max}	ng/mL	92901	15333	10712	1592

^aArea under the curve. ^bArea under the first moment of the plasma concentration–time curve. ^cMean retention time, MRT = AUMC/AUC. ^dTotal body clearance.

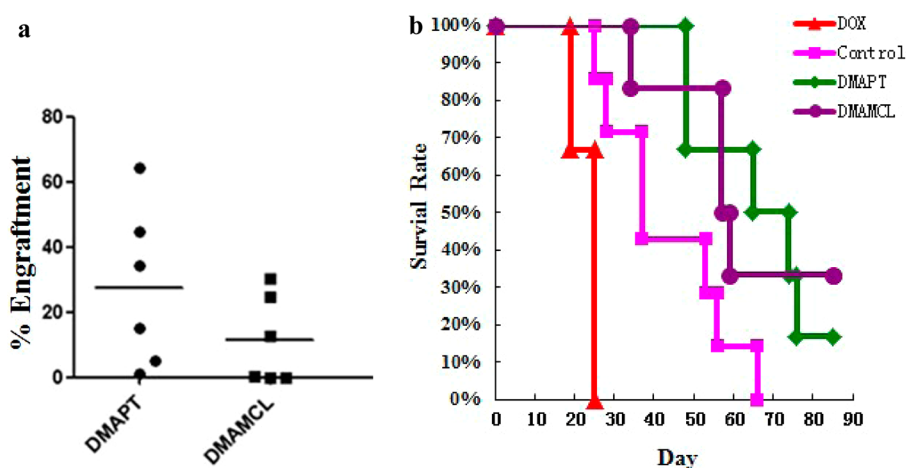


Figure 13. In vivo biological activity of DMAPT in a murine model. (a) Percentage of CD45⁺CD33⁺ cells after treatment with DMAPT (●) and DMAMCL (■). Each ● or ■ symbol represents a single animal. The mean percentage is indicated by the horizontal bars. (b) Kaplan–Meier survival curves, control ($n = 7$), DOX ($n = 6$), DMAPT ($n = 6$), DMAMCL ($n = 6$).

sacrificed in 35 days after the drug treatment, and their bone marrow was analyzed. The average percentage of the CD45⁺CD33⁺ cancer cells in the bone marrow of DMAMCL-treated mice was 0.14%, which was significantly lower than that of DMAPT-treated mice (5.7%). Compared to the average percentage of 9.8% CD45⁺CD33⁺ cells in the bone marrow of the saline-treated control group, there was a 98.6% inhibition of cancer cell engraft for the

DMAMCL group and a 42% inhibition for the DMAPT group (Table 7). These in vivo experimental data demonstrate that DMAMCL was superior to DMAPT in efficacy.

Toxicity Evaluation of Compound DMAMCL. As a preliminary toxicology study, we treated BALB/c mice with DMAMCL and carried out hematoxylin and eosin (H&E) staining of the heart, liver, spleen, lung, and kidney. The animals were given

Table 7. Percentage of CD45⁺CD33⁺ Cells in the Bone Marrow of DMAPT- and DMAMCL-Treated Mice^a

no.	control	DMAPT group	DMAMCL group
1	3.29	2.87	0.02
2	1.6	1.35	0.056
3	5.19	36.9	0.259
4	1.12	1.91	0.177
5	55.1	1.1	0.141
6	0.986	0.74	0.212
7	1.25	0.442	0.221
8	10.8	0.373	N/A
av	9.8	5.7	0.14
AML cell inhibition compared to the control (%)	N/A	42	98.6

^aThe mice were engrafted with primary mixed-lineage leukemia cells.

1000 mg/kg DMAMCL by gavage in a single dose or 500 mg/kg every day for 7 days. No pathologic changes were apparent in the examined tissues (Supporting Information, p S23). This indicates that DMAMCL is well-tolerated by oral administration.

DISCUSSION

Conventional chemotherapies and radiation therapies for cancer usually affect only differentiated or differentiating cells, which form the bulk of the tumor. However, in many cases, a small population of CSCs could remain untouched and cause the relapse of cancer.^{1–4} Unfortunately, only a few compounds can selectively inhibit CSCs and reduce the proportion of CSCs in vitro or in vivo. Parthenolide, a 10,5-ring structure SL, is able to target several types of cancer stem cells,⁹ and its water-soluble analogue, DMAPT, is currently in clinical trial.^{9c}

We found that some GSLs, 5,7,5-ring structure SLs, and their derivatives were able to selectively inhibit AML stem and progenitor cells, including compounds arglabin, **1**, **9** (MCL), **10**, **12**, **19**, and **20**. The cell viabilities of stem/progenitor cells vs total leukemia cells after treatment with these compounds were (arglabin) 10.7% vs 20.0%, (**1**) 3.8% vs 6.4%, (**9**) 2.3% vs 8.4%, (**10**) 44.5% vs 49.7%, (**12**) 22.6% vs 30.6%, (**19**) 2.1% vs 10.8%, and (**20**) 11.2% vs 53.1% (Table 2). We also established the first preliminary SAR against AML stem/progenitor cells (Figure 5). Note that arglabin is an anticancer drug currently being used for treatment of breast, liver, and lung cancers in some countries.²⁴ Further investigation demonstrated that MCL, PTL, and arglabin may selectively kill AML stem cells and then may reduce the proportion of the AML stem cells in overall surviving AML cells (Table 3). The targeting of AML stem/progenitor cells with MCL was confirmed by reduction of the CFUs to the primary AML cells. Moreover, surviving primary AML cells after MCL treatment had significantly low engraftment in mice compared to that of an equal amount of saline-treated primary AML cells (Figure 9).

DMAPT, the water-soluble dimethylamino Michael adduct of PTL, was reported to be equally as potent as PTL in vitro,^{9b} while the Michael adduct of MCL, DMAMCL, was significantly less active in vitro (Tables 1 and 2). However, in neutral HEPES solution (pH 7.4) and in plasma, the conversion of DMAMCL to MCL is much slower than that of DMAPT to PTL (Figures 10 and 11). The preliminary pharmacokinetic (PK) study demonstrated that DMAMCL showed high oral bioavailability and constant conversion to active drug MCL. This phenomenon,

along with the much higher plasma stability of MCL over PTL (half-lives of MCL and PTL in mouse plasma, 2.64 vs 0.36, Table 4), is helpful to control the blood concentration of MCL within a suitable window, which is important to ensure a high AUC and to reduce toxicity (Tables 5 and 6). Moreover, MCL was less toxic to normal cells. In summary, the drug/prodrug form of MCL/DMAMCL had at least three advantages over PTL/DMAPT: higher stability of active drug, less toxic to normal cells and normal stem cells, and more sustainable release of active drug from prodrug. Indeed, 33% of the NOD/SCID mice even survived in a “disease-free” state at the end of the in vivo efficacy study engrafted with M5 AML cells; in comparison, all the DMAPT-treated mice still had a significant percentage of human primary AML cells remaining (Figure 13). In another similar in vivo experiment with engrafted acute mixed-lineage leukemia cells, the percentage of CD45⁺CD33⁺ cells in the bone marrow of DMAMCL-treated mice was significantly lower than that of DMAPT-treated mice; compared to the control group, this is 98.6% inhibition in the DMAMCL group vs 42% inhibition in the DMAPT group (Table 7). This indicates that DMAMCL is also a promising drug candidate for acute mixed-lineage leukemia. Note that acute mixed-lineage leukemia still has a very poor prognosis and still needs an optimal therapeutic approach.²⁵ In addition, the acute toxicity of DMAMCL via oral administration is very low; the maximum tolerable doses (MTDs) of DMAMCL are over 1000 mg/kg for a single dose and 500 mg/kg every day for seven doses, which are 10 times and 5 times the effective dose (100 mg/kg), respectively. However, the MTD for DMAMCL via intravenous (iv) administration is around 200 mg/kg for a single dose (data not shown). This significant difference of MTD between oral and iv administration may be explained by the comparison of pharmacokinetic parameters of DMAMCL after iv and oral administrations (Figure 12). The drug (DMAMCL) blood concentration over time after iv administration is a “peak” and “trough” curve, while sustained absorption and release were observed when DMAMCL was administrated orally. Argabin, an anticancer drug administrated by injection and which is currently in clinical trials in some countries, has a relatively narrow therapeutic index compared to DMAMCL. The LD₅₀ of argabin by intraperitoneal injection is 190–220 mg in mice, and the MTD of argabin by iv administration is around the same range as the effective dose (from 20 to 50 mg/kg daily for 20 days).¹⁸ In summary, the significantly broader therapeutic index is the major advantage of DMAMCL over argabin, and this result also suggests that administration routes may have an important effect on the therapeutic index.

CONCLUSION

As a speculative view, although the cell-based biology of CSCs has been studied intensively, small molecules that can selectively target cancer stem cells are still very rare. The discovery of more agents that selectively inhibit CSCs is highly urgent for studying the specific target mechanisms of CSCs. In this context, the scaffold hopping of the 10,5-ring structure of PTL to the 5,7,5 ring structure of GSLs resulted in the discovery of a library of anti-AML stem/progenitor cell agents, and the lead compound MCL demonstrates higher plasma stability, more sustained release, and superior in vivo efficacy compared to PTL, which may be beneficial to in vivo mechanism investigation. This discovery suggests that GSLs, and probably even all subtypes of SLs, could be a rich source to identify anti-AML stem/progenitor cell agents. Indeed, different types of SLs and their derivatives have been prepared and tested against different types of cancer

stem/progenitor cells. Moreover, molecular probes based on the established SAR of GSLs may be developed and will be applied to identify/confirm their specific target in AML stem cells and other types of CSCs, especially in vivo. All these works will be published in due course.

METHODS

Synthesis of Compounds 8–22. PTL was dissolved in MeOH/H⁺ at room temperature and resulted in the formation of compound 8.²⁶ Cyclization of PTL using BF₃ in toluene provided compounds 9–12.²⁷ Taking into account that the physiological environment is aqueous, the cyclization was carried out in an acetone/water mixture to obtain compound 13.²⁸ Compound 14 is a N₃ adduct of PTL, and compounds 15–18 are the products obtained by Cu(I)-catalyzed reaction of compound 14 with various alkynes (Figure 3). MCL (compound 9) can also be prepared in high yield using our modified method,²⁹ and the derivatives of micheliolide (compounds 19, 20, 21, and 22) were prepared as outlined in Figure 4. MCL was treated with MeI and NaH in THF to provide methylated product 19. Derivative 20 was obtained as a N₃ adduct. Compound 21 (DMAMCL) was obtained as a white powder through dimethylamine addition to MCL,³⁰ followed by addition of 1 equiv of HCl and lipophilization. Hydrogenation of MCL with NaBH₄ formed dihydromicheliolide (compound 22).

Materials and Experimental Procedure of the PK Study. The UPLC–MS/MS system consisted of an AcQuity ultraperformance liquid chromatograph and a Quattro Premier XE mass spectrometer (Waters/Micromass, Milford, MA). All solvents and chemicals were of HPLC grade and purchased from Fisher Scientific (Tustin, CA).

Male Kunming mice (20 ± 2 g) were supplied by the lab animal center of the Academy of Military Medical Science (Beijing, China). The experimental protocol was approved by the Nankai University Ethics Committee for the use of experimental animals and conformed to the Guide for Care and Use of Laboratory Animals. Mice were housed at 22 ± 2 °C and 55 ± 5% relative humidity under a 12 h light–dark cycle. They were fasted for 12 h before drug administration, and water was freely available. DMAMCL aqueous solution was po (150 mg/kg) or iv (100 mg/kg) administered (*n* = 5). The blood samples were collected from the orbital veins at the setting time. All the biological specimens were stored at –80 °C. PK data were generated using noncompartmental analysis.

Release Studies of Prodrug to Active Drug. A 20 μL volume of DMAMCL or DMAPT solution was placed in 980 μL of HEPES at pH 7.4 or mouse blank plasma solution. The tubes were then incubated in a bath incubator at 37 °C. Samples were removed in 10 s, and the concentration of DMAMCL, MCL, DMAPT, and PTL was analyzed by HPLC.

Cell Isolation and Culture. Primary human AML samples were obtained from volunteer donors from the Institute of Hematology & Blood Diseases Hospital (Tianjin, China). Umbilical cord blood samples were obtained from a volunteer donor in the Maternity Hospital (Tianjin, China). Mononuclear cells were isolated from the samples using Ficoll-Paque density gradient separation and cryopreserved in a freezing medium of 90% FBS and 10% dimethyl sulfoxide (DMSO) until use. Cells were cultured in serum-free IMDM for 1 h before treatment by the compounds. All the drug treatments were performed in triplicate. The cell viability assay was carried out using the well-documented (3-(4,5-dimethylthiazol-2-yl)-2,5-diphenyltetrazolium bromide (MTT) method. All the tested cells were cultured with drugs for 72 h before addition of the MTT reagent. All the experiments were carried out in triplicate, and we tested every compound three times.

Methylcellulose Colony-Forming Assay. The mononuclear cells from the cord blood of AML patient volunteers were cultured in serum-free IMDM for 18 h in the presence or absence of drugs. The drug concentrations were 0.05 μM DOX, 0.10 μM DOX, 5 μM PTL, 10 μM PTL, 5 μM MCL, and 10 μM MCL, respectively. Cells were plated in triplicate in the methylcellulose medium M3434 (StemCell Technologies, Vancouver, Canada), and total colonies (CFC-Mix, CFC-granulocyte and -monocyte, CFC-granulocyte, CFC-monocyte/macrophage, and

BFU-erythrocyte) were scored after 20 days of culture. We counted the colonies by the colony morphology.

Flow Cytometry. Apoptosis assays were performed as follows. First, after 18 h of treatment, with the compounds in IMDM, normal and AML samples were isolated and stained by the antibodies CD34-allophycocyanin (APC) and CD38-PECy7 for 30 min. The cells were washed in cold phosphate-buffered saline (PBS) and resuspended in 100 μL of Annexin-V buffer. Annexin-V–fluorescein isothiocyanate (FITC) and propidium iodide (PI) were added, and the tubes were vortexed gently. After that the tubes were incubated at room temperature for 15 min, the samples were analyzed on a BD LSRII flow cytometer (BD Biosciences). We analyzed the data with Prism 5 software.

NOD/SCID Mouse Assays. NOD/SCID mice were sublethally irradiated with 280cGy before transplantation. After 6–10 h, the cells to be assayed (from M5) were injected via tail vein in a final volume of 0.2 mL of PBS. After the cells were transplanted for 8 weeks, DMAMCL and DMAPT (aqueous solution, 100 mg/kg each time) were administered orally every other day. After seven times the administrations were stopped.

Toxicity Evaluation of Compound DMAMCL. Untreated mice and mice treated with the diluent alone (water) were utilized as controls to document the normal tissue architecture and inflammation status in the heart, lung, spleen, and kidney. The experiment was performed with a total of 16 mice (8 male/8 female) at the indicated time point examined. Mice were sacrificed at 1 week after DMAMCL (aqueous solution, 1000 mg/kg for a single dose or 500 mg/kg every day for seven doses) was orally administered, and the entire tissue was surgically excised. All the tissues were fixed in 10% neutral-buffered formalin and embedded in paraffin, and sections of 3 μm thickness were subjected to H&E staining by standard procedures. Gross morphological analyses were performed on tissues stained with H&E. Tissue sections from all mice within a treatment group were visually examined by using an Olympus IX81 microscope to assess the gross morphological condition. After the overall assessment of the tissue, a representative field from the heart, lung, spleen, and kidney of each treatment group was photographed by using a high-resolution digital camera.

ASSOCIATED CONTENT

Supporting Information

Experimental procedure, NMR spectra of compounds 8–22, and pathology pictures. This material is available free of charge via the Internet at <http://pubs.acs.org/>.

AUTHOR INFORMATION

Corresponding Author

*Phone: +86 22 23508090. Fax +86 22 23508090. E-mail: yuechen@nankai.edu.cn (Y.C.); gaoyingdai@hotmail.com (Y.G.).

Author Contributions

#These authors contributed equally to this work.

Notes

The authors declare the following competing financial interest(s): Y.C. is one of the founders of Accendatech Co., Ltd., which has a financial interest in DMAMCL. All other authors declare no competing financial interests.

ACKNOWLEDGMENTS

This work was supported by the National Basic Research Program of China (Grants 2011CB964801 and 2012CB966604), the National Natural Science Foundation of China (NSFC) (Grants 21072106 to Y.C., 81001377 to Q.Z., 90913018, 81090410, and 81170465), The Ministry of Science and Technology (Grant 2009CB918901), the Fok Ying Tong Education Foundation (Grant 122037), and The Natural Science Foundation of Tianjin (TJNSF) (Grant 09JCZDJC21900).

■ ABBREVIATIONS USED

CSC, cancer stem cell; PTL, parthenolide; SL, sesquiterpene lactone; SERCA, sarco/endoplasmic reticulum calcium transport ATPase; LSC, leukemia stem cell; BCSC, breast cancer stem cell; GSL, guaianolide sesquiterpene lactone; DMAPT, (dimethylamino)parthenolide; MCL, micheliolide; DMAMCL, (dimethylamino)micheliolide; NOD/SCID, nonobese diabetic/severe combined immunodeficiency; DOX, doxorubicin; HSC, hematopoietic stem/progenitor cell; CFU, colony-forming unit; AUMC, area under the first moment of the plasma concentration–time curve; MRT, mean retention time, $MRT = AUMC/AUC$; CL, total body clearance

■ REFERENCES

- (1) (a) Lapidot, T.; Sirard, C.; Vormoor, J.; Murdoch, B.; Hoang, T.; Caceres-Cortes, J.; Minden, M.; Paterson, B.; Caligiuri, M. A.; Dick, J. E. A cell initiating human acute myeloid leukaemia after transplantation into SCID mice. *Nature* **1994**, *367*, 645–648. (b) Bonnet, D.; Dick, J. E. Human acute myeloid leukemia is organized as a hierarchy that originates from a primitive hematopoietic cell. *Nat. Med.* **1997**, *3*, 730–737. (c) Stefanachi, A.; Leonetti, F.; Nicolotti, O.; Catto, M.; Pisani, L.; Cellamare, S.; Altomare, C.; Carotti, A. New strategies in the chemotherapy of leukemia: eradicating cancer stem cells in chronic myeloid leukemia. *Curr. Cancer Drug Targets* **2012**, *12*, 571–596.
- (2) (a) Singh, S. K.; Hawkins, C.; Clarke, I. D.; Squire, J. A.; Bayani, J.; Hide, T.; Henkelman, R. M.; Cusimano, M. D.; Dirks, P. B. Tissue repair and stem cell renewal in carcinogenesis. *Nature* **2004**, *432*, 396–401. (b) Singh, S. K.; Clarke, I. D.; Terasaki, M.; Bonn, V. E.; Hawkins, C.; Squire, J.; Dirks, P. B. Identification of a cancer stem cell in human brain tumors. *Cancer Res.* **2003**, *63*, 5821–5828. (c) Al-Hajj, M.; Wicha, M. S.; Benito-Hernandez, A.; Morrison, S. J.; Clarke, M. F. Prospective identification of tumorigenic breast cancer cells. *Proc. Natl. Acad. Sci. U.S.A.* **2003**, *100*, 3983–3988. (d) O'Brien, C. A.; Pollett, A.; Gallinger, S.; Dick, J. E. A human colon cancer cell capable of initiating tumour growth in immunodeficient mice. *Nature* **2007**, *445*, 106–110. (e) Zhang, S.; Balch, C.; Chan, M. W.; Lai, H. C.; Matei, D.; Schilder, J. M.; Yan, P. S.; Huang, T. H.; Nephew, K. P. Identification and characterization of ovarian cancer-initiating cells from primary human tumors. *Cancer Res.* **2008**, *68*, 4311–4320. (f) Li, C.; Heidt, D. G.; Dalerba, P.; Burant, C. F.; Zhang, L.; Adsay, V.; Wicha, M.; Clarke, M. F.; Simeone, D. M. Identification of pancreatic cancer stem cells. *Cancer Res.* **2007**, *67*, 1030–1037. (g) Maitland, N. J.; Collins, A. T. Prostate cancer stem cells: a new target for therapy. *J. Clin. Oncol.* **2008**, *26*, 2862–2870. (h) Lang, S. H.; Frame, F.; Collins, A. Prostate cancer stem cells. *J. Pathol.* **2009**, *217*, 299–306. (i) Schatton, T.; Murphy, G. F.; Frank, N. Y.; Yamaura, K.; Waaga-Gasser, A. M.; Gasser, M.; Zhan, Q.; Jordan, S.; Duncan, L. M.; Weishaupt, C.; Fuhlbrigge, R. C.; Kupper, T. S.; Sayegh, M. H.; Frank, M. H. Identification of cells initiating human melanomas. *Nature* **2008**, *451*, 345–349. (j) Boiko, A. D.; Razorenova, O. V.; van de Rijn, M.; Swetter, S. M.; Johnson, D. L.; Ly, D. P.; Butler, P. D.; Yang, G. P.; Joshua, B.; Kaplan, M. J.; Longaker, M. T.; Weissman, I. L. Human melanoma-initiating cells express neural crest nerve growth factor receptor CD271. *Nature* **2010**, *466*, 133–137. (k) Schmidt, P.; Kopecky, C.; Hombach, A.; Zigrino, P.; Mauch, C.; Abken, H. *Proc. Natl. Acad. Sci. U.S.A.* **2011**, *108*, 2474–2479. (l) Civenni, G.; Walter, A.; Kobert, N.; Mihic-Probst, D.; Zipser, M.; Belloni, B.; Seifert, B.; Moch, H.; Dummer, R.; van den Broek, M.; Sommer, L. Human CD271-positive melanoma stem cells associated with metastasis establish tumor heterogeneity and long-term growth. *Cancer Res.* **2011**, *71*, 3098–3109.
- (3) (a) Abbott, A. The root of the problem. *Nature* **2006**, *442*, 742–743. (b) Chen, B.; Dodge, M. E.; Tang, W.; Lu, J.; Ma, Z.; Fan, C.-W.; Wei, S.; Hao, W.; Kilgore, J.; Williams, N. S.; Roth, M. G.; Amatruda, J. F.; Chen, C.; Lum, L. Small molecule-mediated disruption of Wnt-dependent signaling in tissue regeneration and cancer. *Nat. Chem. Biol.* **2009**, *5*, 100–107. (c) Orkin, S. H.; Zon, L. I. An evolving paradigm for stem cell biology. *Cell* **2008**, *132*, 631–644. (d) Shen, H.-M.; Tergaonker, V. NF κ B signaling in carcinogenesis and as a potential molecular target for cancer therapy. *Apoptosis* **2009**, *14*, 348–363. (e) Odoux, C.; Fohrer, H.; Hoppe, T.; Guzik, L.; Stolz, D. B.; Lagasse, E. A. Stochastic model for cancer stem cell origin in metastatic colon cancer. *Cancer Res.* **2008**, *68*, 6932–6941. (f) Savona, M.; Talpaz, M. *Nat. Rev. Cancer* **2008**, *8*, 341–350. (g) Rossi, D. J.; Jamieson, C. H. M.; Weissman, I. L. Getting to the stem of chronic myeloid leukaemia. *Cell* **2008**, *132*, 681–696.
- (4) (a) Gupta, P. B.; Onder, T. T.; Jiang, G.; Tao, K.; Kuperwasser, C.; Weinberg, R. A.; Lander, E. S. Identification of selective inhibitors of cancer stem cells by high-throughput screening. *Cell* **2009**, *138*, 645–659. (b) Bao, S.; Wu, Q.; McLendon, R. E.; Hao, Y.; Shi, Q.; Hjelmeland, A. B.; Dewhirst, M. W.; Bigner, D. D.; Rich, J. N. Glioma stem cells promote radioresistance by preferential activation of the DNA damage response. *Nature* **2006**, *444*, 756–760. (c) Dean, M.; Fojo, T.; Bates, S. Tumour stem cells and drug resistance. *Nat. Rev. Cancer* **2005**, *5*, 275–284. (d) Diehn, M.; Clarke, M. F. Cancer stem cells and radiotherapy: new insights into tumor radioresistance. *J. Natl. Cancer Inst.* **2006**, *98*, 1755–1757. (e) Eyler, C. E.; Rich, J. N. Survival of the fittest: cancer stem cells in therapeutic resistance and angiogenesis. *J. Clin. Oncol.* **2008**, *26*, 2839–2845. (f) Li, X.; Lewis, M. T.; Huang, J.; Gutierrez, C.; Osborne, C. K.; Wu, M. F.; Hilsenbeck, S. G.; Pavlick, A.; Zhang, X.; Chamness, G. C.; Wong, H.; Rosen, J.; Chang, J. C. Intrinsic resistance of tumorigenic breast cancer cells to chemotherapy. *J. Natl. Cancer Inst.* **2008**, *100*, 672–679. (g) Woodward, W. A.; Chen, M. S.; Behbod, F.; Alfaro, M. P.; Buchholz, T. A.; Rosen, J. M. WNT/ β -catenin mediates radiation resistance of mouse mammary progenitor cells. *Proc. Natl. Acad. Sci. U.S.A.* **2007**, *104*, 618–623.
- (5) Chakraborty, S.; Kanakasabai, S.; Bright, J. J. Constitutive androstane receptor agonist CITCO inhibits growth and expansion of brain tumor stem cells. *Br. J. Cancer* **2011**, *104*, 448–459.
- (6) Ginestier, C.; Liu, S.; Diebel, M. E.; Korkaya, H.; Luo, M.; Brown, M.; Wicinski, J.; Cabaud, O.; Charafe-Jauffret, E.; Birnbaum, D.; Guan, J. L.; Dontu, G.; Wicha, M. CXCR1 blockade selectively targets human breast cancer stem cells *in vitro* and in xenografts. *S. J. Clin. Invest.* **2010**, *120*, 485–497.
- (7) Zhou, J.; Zhang, H.; Gu, P.; Bai, J.; Margolick, J. B.; Zhang, Y. NF- κ B pathway inhibitors preferentially inhibit breast cancer stem-like cells. *Breast Cancer Res. Treat.* **2008**, *111*, 419–427.
- (8) Li, Y.; Zhang, T.; Korkaya, H.; Liu, S.; Lee, H.-F.; Newman, B.; Yu, Y.; Clouthier, S. G.; Schwartz, S. J.; Wicha, M. S.; Sun, D. Intrinsic resistance of tumorigenic breast cancer cells to chemotherapy. *Clin. Cancer Res.* **2010**, *16*, 2580–2590.
- (9) (a) Guzman, M. L.; Rossi, R. M.; Karnischky, L.; Li, X.; Peterson, D. R.; Howard, D. S.; Jordan, C. T. The sesquiterpene lactone parthenolide induces apoptosis of human acute myelogenous leukemia stem and progenitor cells. *Blood* **2005**, *105*, 4163–4169. (b) Guzman, M. L.; Rossi, R. M.; Neelakantan, S.; Li, X.; Corbett, C. A.; Hassane, D. C.; Becker, M. W.; Bennett, J. M.; Sullivan, E.; Lachowicz, J. L.; Vaughan, A.; Sweeney, C. J.; Matthews, W.; Carroll, M.; Liesveld, J. L.; Crooks, P. A.; Jordan, C. T. An orally bioavailable parthenolide analog selectively eradicates acute myelogenous leukemia stem and progenitor cells. *Blood* **2007**, *110*, 4227–4435. (c) Ghantous, A.; Gali-Muhtasib, H.; Vuorela, H.; Saliba, N. A.; Darwiche, N. What made sesquiterpene lactones reach cancer clinical trials? *Drug Discovery Today* **2010**, *15*, 668–678. (d) Liu, Y.; Lu, W. L.; Guo, J.; Du, J.; Li, T.; Wu, J. W.; Wang, G. L.; Wang, J. C.; Zhang, X.; Zhang, Q. A potential target associated with both cancer and cancer stem cells: A combination therapy for eradication of breast cancer using vinorelbine stealthy liposomes plus parthenolide stealthy liposomes. *J. Controlled Release* **2008**, *129*, 18–25. (e) Kawasaki, B. T.; Hurt, E. M.; Kalathur, M.; Duhagon, M. A.; Milner, J. A.; Kim, Y. S.; Farrar, W. L. Effects of the sesquiterpene lactone parthenolide on prostate tumor-initiating cells: An integrated molecular profiling approach. *Prostate* **2009**, *67*, 827–837. (f) Neelakantan, S.; Nasim, S.; Guzman, M. L.; Jordan, C. T.; Crooks, P. A. Aminoparthenolide as novel anti-leukemic agents: discovery of the NF- κ B inhibitor, DMAPT (LC-1). *Bioorg. Med. Chem. Lett.* **2009**, *19*, 4346–4349. (g) Kevin, P. New agents for the treatment of leukemia: discovery of DMAPT (LC-1). *Drug Discovery Today* **2010**, *15*, 322.

- (10) Li, X.; Lewis, M. T.; Huang, J.; Gutierrez, C.; Osbome, C. K.; Wu, M. F.; Hilsenbeck, S. G.; Pavlick, A.; Zhang, X.; Chamness, G. C.; Wong, H.; Rosen, J.; Chang, J. C. Intrinsic resistance of tumorigenic breast cancer cells to chemotherapy. *J. Natl. Cancer Inst.* **2008**, *100*, 672–679.
- (11) (a) Jordan, C. T. Cancer stem cell biology: from leukemia to solid tumors. *Curr. Opin. Cell Biol.* **2004**, *16*, 708–712. (b) Hemmati, H. D.; Nakano, I.; Lazareff, J. A.; Masterman-Smith, M.; Geschwind, D. H.; Bronner-Fraser, M.; Kornblum, H. I. Cancerous stem cells can arise from pediatric brain tumors. *Proc. Natl. Acad. Sci. U.S.A.* **2003**, *100*, 15178–15183. (c) Diévert, A.; Beaulieu, N.; Jolicœur, P. Involvement of Notch1 in the development of mouse mammary tumors. *Oncogene* **1999**, *18*, 5973–5981. (d) Beachy, P. A.; Karhadkar, S. S.; Berman, D. M. Tissue repair and stem cell renewal in carcinogenesis. *Nature* **2004**, *432*, 324–331. (e) Bollmann, F. M. The many faces of telomerase: emerging extratelomeric effects. *BioEssays* **2008**, *30*, 728–732.
- (12) (a) Gopal, Y. V.; Arora, T. S.; Van Dyke, M. W. Parthenolide specifically depletes histone deacetylase 1 protein and induces cell death through ataxia telangiectasia mutated. *Chem. Biol.* **2007**, *14*, 813–823. (b) Kim, Y. J.; Choi, M. H.; Hong, S. T.; Bae, Y. M. Resistance of cholangiocarcinoma cells to parthenolide-induced apoptosis by the excretorysecretory products of *Clonorchis sinensis*. *Parasitol. Res.* **2009**, *104*, 1011–1016. (c) Riganti, C.; Doublier, S.; Viariso, D.; Miraglia, E.; Pescarmona, G.; Ghigo, D.; Bosia, A. Artemisinin induces doxorubicin resistance in human colon cancer cells via calcium-dependent activation of HIF-1 α and P-glycoprotein overexpression. *Br. J. Pharmacol.* **2009**, *156*, 1054–1066. (d) Dell'Agli, M.; Galli, G. V.; Bosio, E.; Dambrosi, M. Inhibition of NF- κ B and metalloproteinase-9 expression and secretion by parthenolide derivatives. *Bioorg. Med. Chem. Lett.* **2009**, *19*, 1858–1860.
- (13) Guzman, M. L.; Neering, S. J.; Upchurch, D.; Grimes, B.; Howard, D. S.; Rizzieri, D. A.; Luger, S. M.; Jordan, C. T. Nuclear factor- κ B is constitutively activated in primitive human acute myelogenous leukemia cells. *Blood* **2001**, *98*, 2301–2307.
- (14) (a) Merfort, I. Perspective on sesquiterpene lactones in inflammation and cancer. *Curr. Drug Targets* **2011**, *12*, 1560–1573. (b) Woods, J. R.; Mo, H.; Beiberch, A. A.; Alavanjac, T.; Colby, D. A. Amino-derivatives of the sesquiterpene lactone class of natural products as prodrugs. *Med. Chem. Commun.* **2012**, in press.
- (15) Hehner, S. P.; Heinrich, M.; Bork, P. M.; Vogt, M.; Ratter, F.; Lehmann, V.; Schulze-Osthoff, K.; Dröge, W.; Schmitz, M. L. Sesquiterpene lactones specifically inhibit activation of NF- κ B by preventing the degradation of I κ B- α and I κ B- β . *J. Biol. Chem.* **1998**, *273*, 1288–1297.
- (16) Jin, P.; Madieh, S.; Augsburg, L. L. The solution and solid state stability and excipient compatibility of parthenolide in feverfew. *AAPS PharmSciTech* **2007**, *8*, 200–205.
- (17) Schall, A.; Reiser, O. Synthesis of biologically active guaianolides with a trans-annulated lactone moiety. *Eur. J. Org. Chem.* **2008**, 2353–2364.
- (18) (a) Adekenov, S. M.; Mukhametzhonov, M. N.; Kagarlitskii, A. D.; Kupriyanov, A. N. Argabin—a new sesquiterpene lactone from *Artemisia glabella*. *Khim. Prir. Soedin.* **1982**, *5*, 655–656. (b) Kalidindi, S.; Jeong, W. B.; Schall, A.; Bandichhor, R.; Nosse, B.; Reiser, O. Enantioselective synthesis of argabin. *Angew. Chem., Int. Ed.* **2007**, *46*, 6361–6363.
- (19) O'Neill, P. M.; Posner, G. H. A medicinal chemistry perspective on artemisinin and related endoperoxides. *J. Med. Chem.* **2004**, *47*, 2945–2964.
- (20) Baeuerle, P. A.; Baltimore, D. Activation of DNA-binding activity in an apparently cytoplasmic precursor of the NF- κ B transcription factor. *Cell* **1988**, *53*, 211–217.
- (21) Ruben, S. M.; Dillon, P. J.; Schreck, R.; Henkel, T.; Chen, C. H.; Maher, M.; Baeuerle, P. A.; Rosen, C. A. Isolation of a rat-related human cDNA that potentially encodes the 65-kD subunit of NF- κ B. *Science* **1991**, *251*, 1490–1493.
- (22) Schmitz, M. L.; Baeuerle, P. A. The p65 subunit is responsible for the strong transcription activating potential of NF- κ B. *EMBO J.* **1991**, *10*, 3805–3817.
- (23) Barthel, B. L.; Zhang, Z.; Rudnicki, D. L.; Coldren, C. D.; Polinkovsky, M.; Sun, H.; Koch, G. G.; Chan, D. C. F.; Koch, T. H. Preclinical efficacy of a carboxylesterase 2-activated prodrug of doxazolidine. *J. Med. Chem.* **2009**, *52*, 7678–7688.
- (24) Shaikenov, T. E.; Adekenov, S. M.; Williams, R. M.; Prashad, N.; Baker, F. L.; Newman, R. Argabin-DMA, a plant derived sesquiterpene, inhibits farnesyltransferase. *Oncol. Rep.* **2001**, *8*, 173–179.
- (25) (a) Rubnitz, J. E.; Onciu, M.; Pounds, S.; Shurtleff, S.; Cao, X.; Raimondi, S. C.; Behm, F. G.; Campana, D.; Razzouk, B. I.; Ribeiro, R. C.; Downing, J. R.; Pui, C. H. Acute mixed lineage leukemia in children: the experience of St Jude Children's Research Hospital. *Blood* **2009**, *113*, 5083–5089. (b) Legrand, O.; Perrot, J. Y.; Simonin, G.; Baudard, M.; Cadiou, M.; Blanc, C.; Ramond, S.; Viguié, F.; Marie, J. P.; Zittoun, R. Adult biphenotypic acute leukaemia: an entity with poor prognosis which is related to unfavourable cytogenetics and P-glycoprotein overexpression. *Br. J. Haematol.* **1998**, *100*, 147–155.
- (26) Neukirch, H.; Kaneider, N. C.; Wiedermann, C. J.; Guerriero, A.; D'Ambrosio, M. Parthenolide and its photochemically synthesized 1(10)Z isomer: chemical reactivity and structure-activity relationship studies in human leucocyte chemotaxis. *Bioorg. Med. Chem.* **2003**, *11*, 1503–1510.
- (27) Castañeda-Acosta, J.; Fischer, N. H.; Vargas, D. Biomimetic transformations of parthenolide. *J. Nat. Prod.* **1993**, *56*, 90–98.
- (28) Jacobsson, U.; Kumar, V.; Saminathan, S. Sesquiterpene lactones from *Michelia champaca*. *Phytochemistry* **1995**, *39*, 839–843.
- (29) Zhai, J.-D.; Li, D.; Long, J.; Zhang, H.-L.; Lin, J.-P.; Qiu, C.-J.; Zhang, Q.; Chen, Y. Biomimetic semisynthesis of argabin from parthenolide. *J. Org. Chem.* **2012**, *77*, 7103–7107.
- (30) Chen, Y.; Zhang, Q.; Zhai, J. D.; Ma, W. W.; Fan, H. X.; Zhang, F. W. C. N. Patent 201,010,153,701.0, Apr 23, 2010.